FIGURES

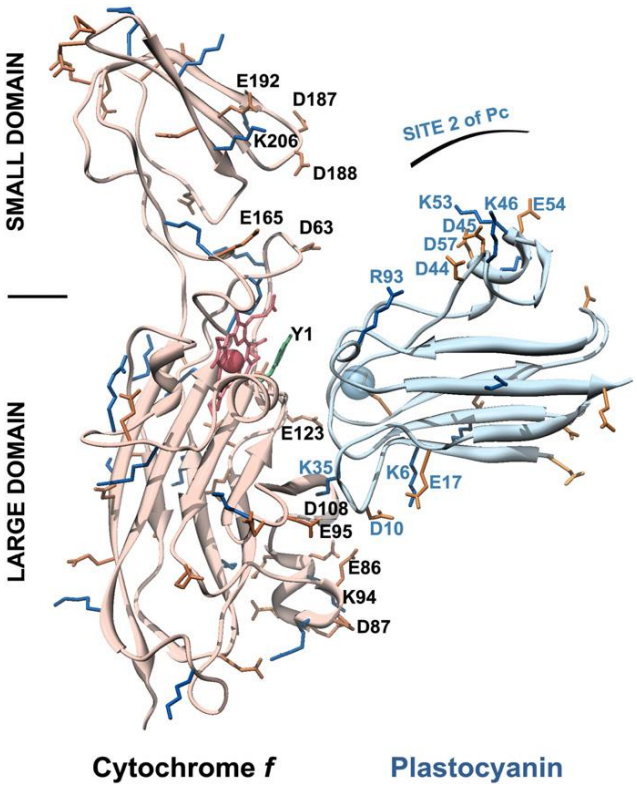

Fig. 1. Robertson diagram of the Pc–C*f* complex of *Phormidium*, based on the NMR structure [29]. Coordinates correspond to the first model in the pdb file. Cf is coloured in pink, Pc is coloured in cyan. Large and small domains of C*f*, as well as site 2 of Pc are explicitly labelled in the figure. Site 1 of Pc corresponds to the interaction surface of this protein in the complex, which locates near the copper site, represented as a cyan sphere. Heme group of C*f* is shown in red sticks. Charged residues from Pc and C*f*, which lie in regions involved in electrostatic interactions with the corresponding partner, are labelled in cyan and black, respectively.

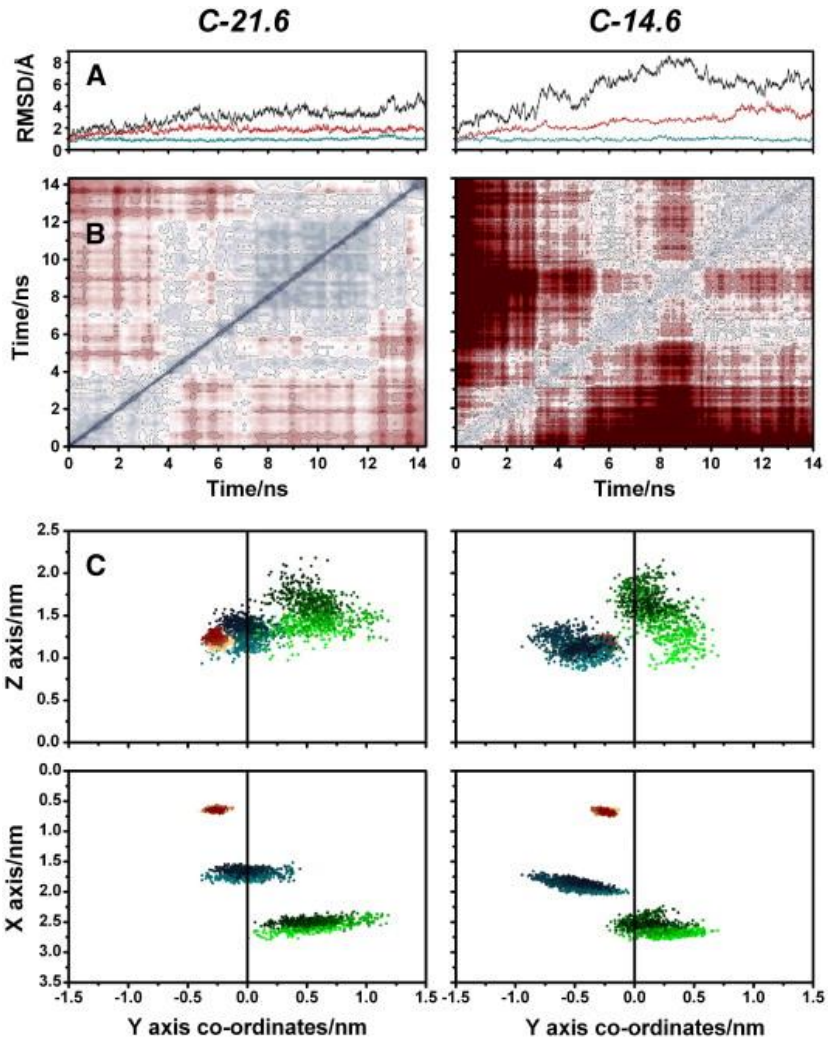

Fig. 2. Molecular dynamics trajectories of the complex between Pc and C*f*. From top to bottom: A) Time evolution of backbone RMSDs with respect to the initial, energy-minimised structures for *C-21.6* (left) and *C-14.6* (right) trajectories. Red lines correspond to C*f*, data from Pc are in cyan; data in black were obtained by aligning the large domain of C*f* and measuring the backbone RMSDs of Pc. B) The two RMSD matrixes of the *C-21.6* (left panels) and the *C-14.6* (right panels) conformations chosen from the NMR data sets. Colour scales correspond to RMSD values from 0 (blue) to 2 Å (white) and from 2Å to 5Å (red). Contours indicate 1, 2, 3 and 4 Å levels. C) Evolution of the complex geometry between Pc and C*f* along the MD trajectories. Figure represents dihedral first angle projections of the trajectories of iron from C*f* (brown dots), copper (blue dots) and centre of mass of Pc (green dots), using the main axes and mass centre of the large domain of C*f* as reference coordinate system: *Z*, *Y* and *X* correspond to the main, secondary and tertiary rotation axes. Left panels show data of the *C-21.6* ensemble. Right panels correspond to the trajectory of the *C-14.6* conformation. Colours shift from light to dark to illustrate changes during the simulation.

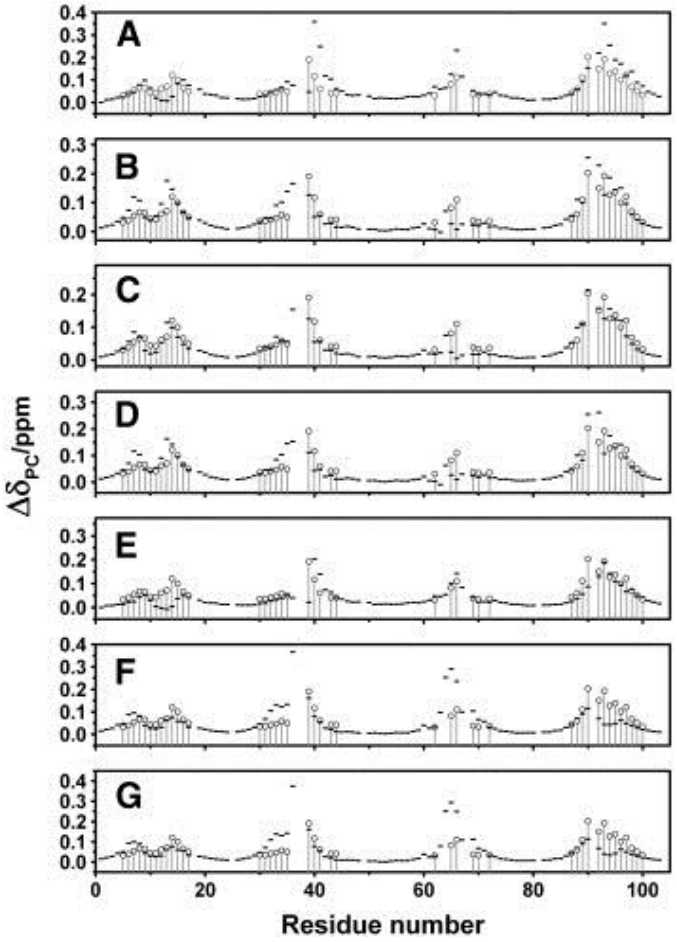

Fig. 3. Validation of trajectories against experimental PS of amide protons. Open circles with drop lines represent PS of amide protons of Pc reported by Crowley et al. [29]. Slash symbols represent average PS calculated from different coordinate sets: A) the selected structure from the NMR ensemble [29] used as a starting point for the *C-21.6* trajectory; B) ensemble of the full *C-21.6* trajectory; C) structures from the time interval between 1 and 4 ns of the *C-21.6* trajectory; D) structures from the time interval between 6 and 13 ns of the *C-21.6* trajectory; E) structure from the NMR ensemble [29], which was used as a starting point for the *C-14.6* simulation; F) ensemble of the full *C-14.6* simulation; G) ensemble of the last 2 ns of the *C-14.6* calculations, the only time interval in which the trajectory was stable, as shown in Fig. 2B, left panel.

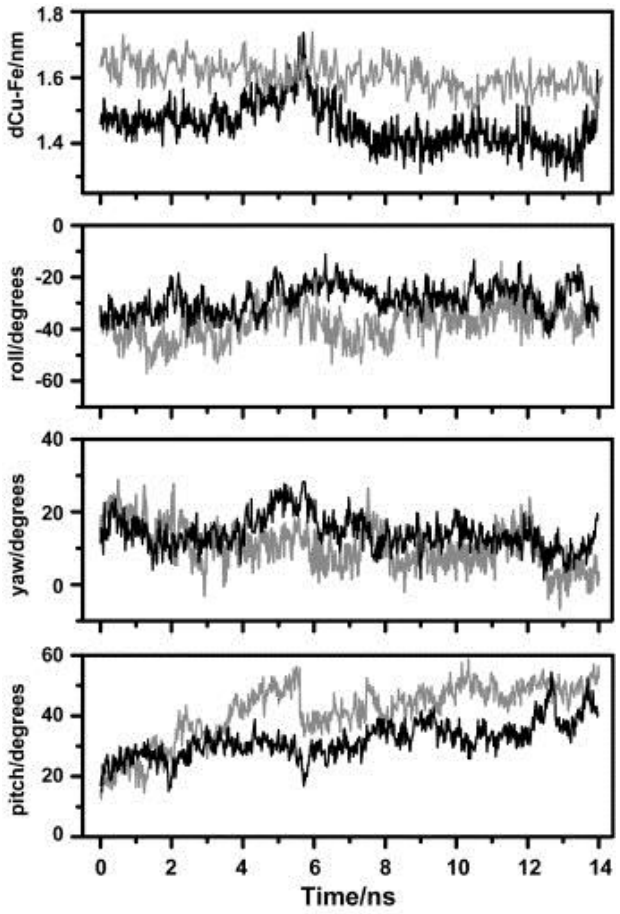

Fig. 4. Geometry of the complex between Pc and C*f* along the MD trajectories. *C-14.6* and *C-21.6* trajectories are coloured by grey and black lines, respectively. Upper panel represents the distance between the metal atoms of the two protein partners. The rest of the panels correspond to orientation angles of the main axes of the small domain of C*f* and Pc with respect to the main axes of the large domain of C*f*. As pointed out in Methods, the perpendicular orientation between the main axes of the two partners is characterised by a zero degree pitch.

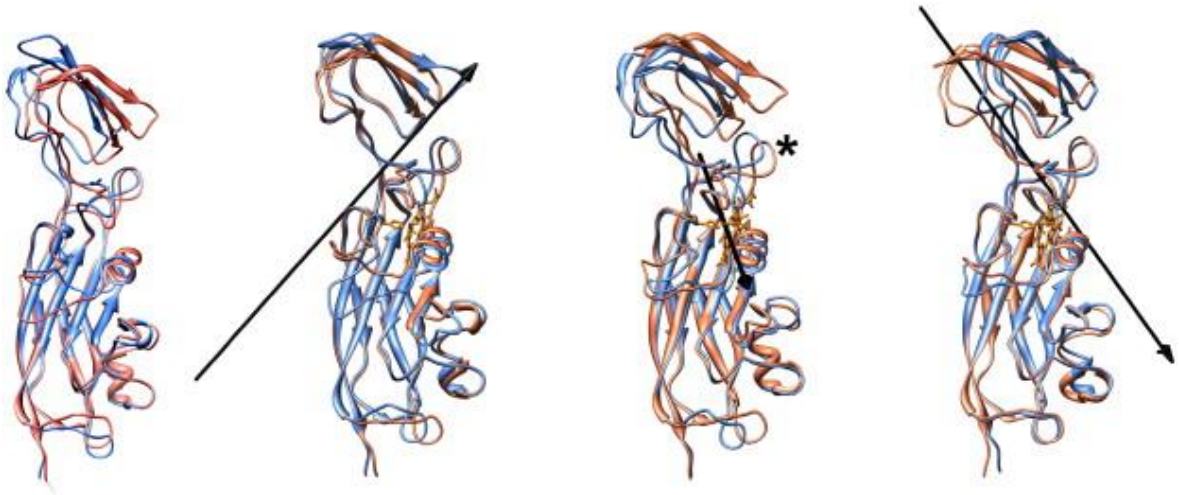

Fig. 5. Domain motions in C*f*. From left to right: ribbons illustrate extreme coordinates – coloured in blue and red – of the four higher amplitude eigenvectors (PC1, PC2, PC3 and PC4, respectively) calculated from the 5 ns trajectory of isolated C*f*. The black arrows correspond to the hinge axes of the domain motion in each case, as calculated with Dyndom [53]. Note that no specific hinge axis was found for the first eigenvector with the parameters tested. The C*f* loop between residues 154 and 171 is labelled with an asterisk (*) symbol.

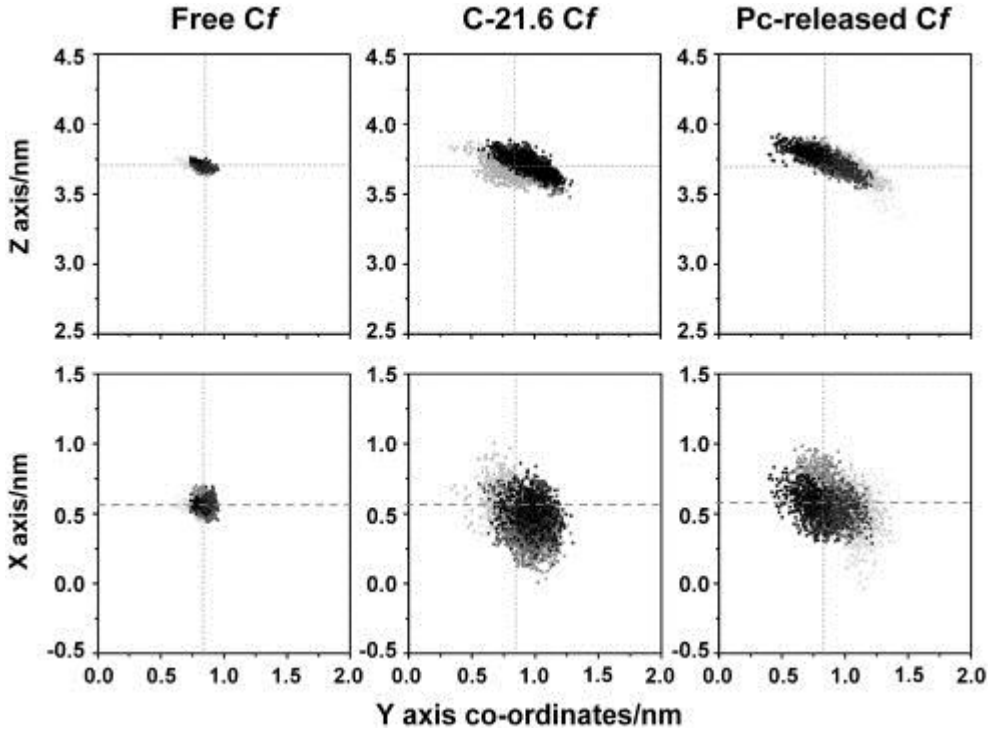

Fig. 6. Conformation changes of C*f* induced by binding of Pc. Figure represents dihedral projections of the trajectories of the mass centre of the small domain of C*f*, using the main axes and mass centre of the large domain of C*f* as reference coordinate system in a similar way as in Fig. 2C. Left: A 5 ns trajectory of C*f*; middle: 14 ns *C-21.6* Pc–C*f* complex; right: 9.8 ns of a MD trajectory of "released" C*f*, wherein starting coordinates were picked out from a snapshot taken at 5 ns of the MD calculation corresponding to the *C-21.6* Pc–C*f* complex. Colour scales from light grey to black illustrate changes during simulation time.

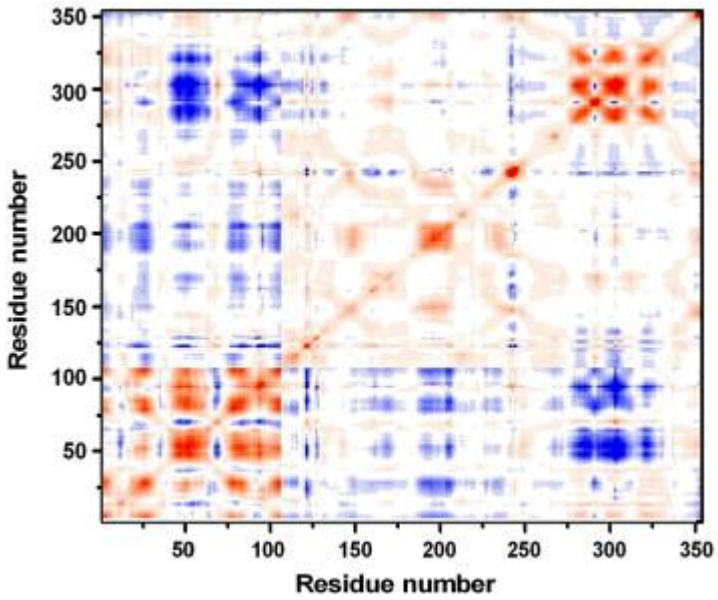

Fig. 7. Coordinate covariance matrix of the trajectory corresponding to the *C-21.6* orientation of the Pc–C*f* complex. The (1062 × 1062) matrix corresponds to covariances of *x*, *y*, and *z* coordinates of protein Cα atoms, and it was obtained after aligning mainchain atoms of the large domain of C*f*. Residues 1 to 105 correspond to Pc, and 106 to 354 to C*f*. Positive values are in red, while negative are coloured in blue.

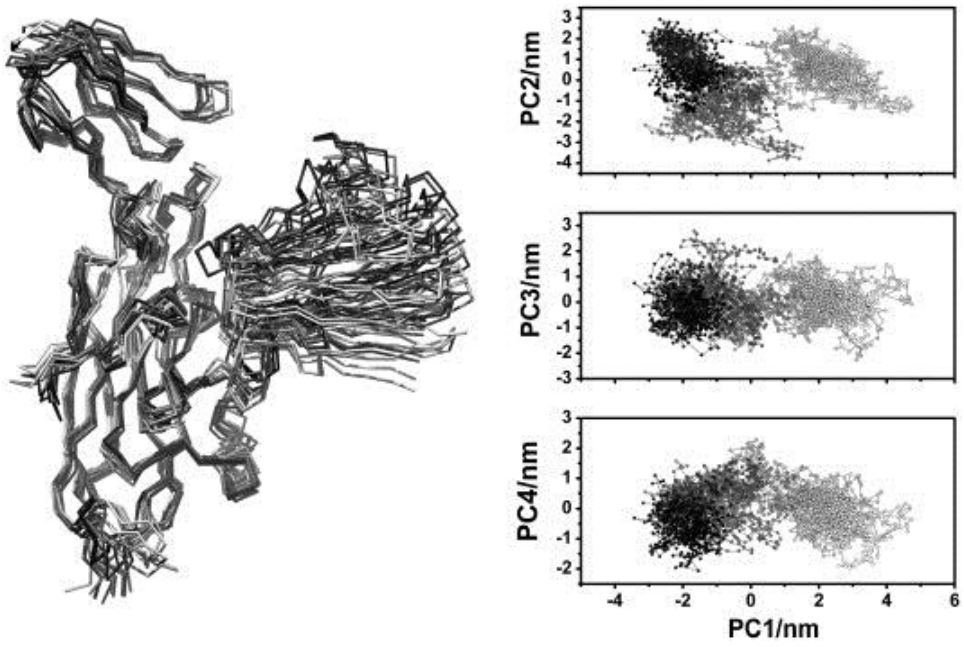

Fig. 8. Principal component analysis of the full *C-21.6* trajectory. Left: Alpha carbon traces of the Pc–C*f* corresponding to the projection of the *C-21.6* trajectory on its first principal component. Right, projection of the trajectory on planes defined by the first eigenvector and the three following ones. Colour shifts from light grey to black along the simulation.

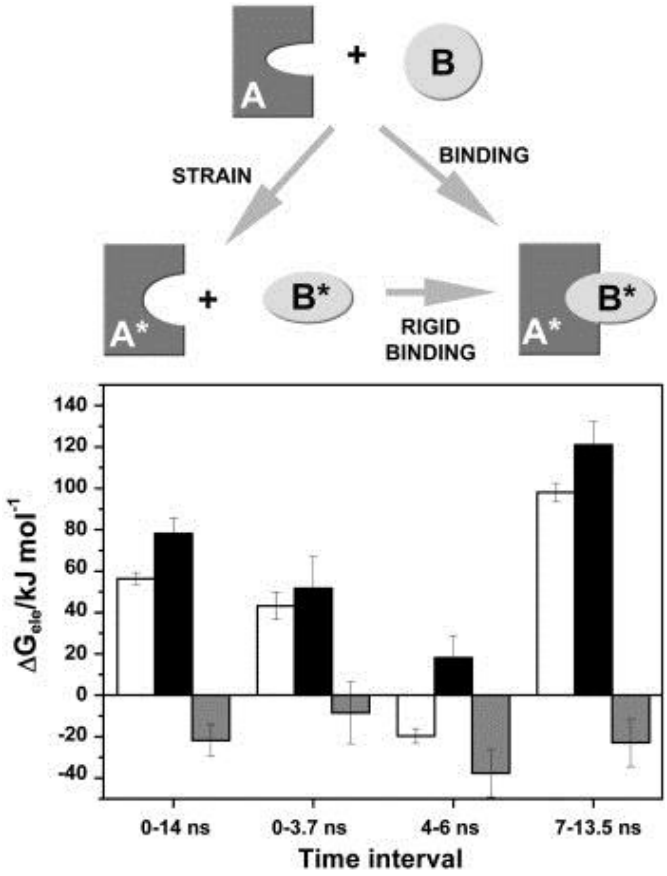

Fig. 9. Electrostatic calculations along the *C-21.6* trajectory. Upper panel: Sheinerman's thermodynamic cycle [56] that describes the binding process. The electrostatic part of the binding free energy, $\Delta G_{\text{ele-bind}}$, is described as a sum of free energies that account for distorting the free monomers to get the conformation they adopt in the complex, $\Delta G_{\text{ele-strain}}$, and their subsequent rigid-body association, $\Delta G_{\text{ele-rigid}}$. Lower panel: Evolution of $\Delta G_{\text{ele-bind}}$ and its components during the full *C-21.6* trajectory and for the different time intervals sampled in these calculations. $\Delta G_{\text{ele-bind}}$ is represented by open bars; $\Delta G_{\text{ele-strain}}$ by black-filled bars; $\Delta G_{\text{ele-rigid}}$ bars are coloured in grey.

TABLE

Table 1. Statistics[a] of generic properties of Pc, C*f*, and their two simulated complexes along MD trajectories.

Trajectory, alignment and analysis	**Time (ns)**	**Average RMSD (Å)**	**Maximum RMSD (Å)**	**Average RMSD drift (pm ns^{-1})**	**Average RMSF (Å)**	**<R_G> (Å)**
C-21.6	13.97					
Pc + C*f*		3.042	5.299	15.90	1.510	24.39
Pc		0.962	1.524	1.28	0.613	13.16
C*f*		1.789	2.625	1.65	1.208	23.21
LD[b]		1.636	2.209	5.70	0.944	17.72
SD[b]		1.150	2.012	5.17	0.790	11.49
C-14.6	13.95					
Pc + C*f*		5.367	8.425	32.61	1.754	24.40
Pc		0.965	1.378	0.57	0.589	13.13
C*f*		2.549	4.493	9.4	1.591	23.41
LD		2.331	3.189	14.5	1.099	17.73
SD		1.064	1.905	4.03	0.733	11.48
Free C*f*	5.00					
C*f*		1.779	3.231	2.34	0.802	22.89
LD		0.763	0.965	7.14	0.414	17.30
SD		0.763	0.946	0.03	0.396	11.11
Pc-released C*f*	9.80					
C*f*		2.019	3.151	7.01	1.169	23.41
LD		1.664	2.464	8.02	0.934	17.87
SD		1.048	1.708	− 0.003	0.72588	11.24
Free Pc	5.00	0.759	1.077	1.26	0.505	13.09

[a] RMSD, root mean square deviation with respect to the initial, energy-minimised structure. RMSD drift values were calculated from linear regressions. They show an error of ca. 10%. RMSFs are root mean square fluctuations of Cα atoms with respect to their average position.⟨ R_G⟩ are the average radii of gyration along the trajectory. Standard errors in this parameter are in the order of 10^{-3} Å.

[b] LD: Large domain of C*f* (residues 1 to 169 and 233 to 247); SD: small domain of C*f* (residues 170 to 232).